Leading Edge Vortex Flow Computations and Comparison with DNW-HST Wind Tunnel Data*)

F.J. Brandsma, H.S. Dol
National Aerospace Laboratory NLR
Applied Aerodynamics Dept.
P.O. Box 90502
1006 BM Amsterdam
The Netherlands

A. Elsenaar
National Aerospace Laboratory NLR
Anthony Fokkerweg 2
1059 CM Amsterdam
The Netherlands

J.C. Kok
National Aerospace Laboratory NLR
Mathematical Methods and Models Dept.
Anthony Fokkerweg 2
1059 CM Amsterdam
The Netherlands

Summary

Computations are presented for the vortical flow around a sharp-edged cropped delta wing with 65° leading edge sweep using a computational method based on the Reynolds-averaged Navier-Stokes equations. It is demonstrated that turbulence modelling plays a crucial role in the ability to capture the vortical structures. Standard one- and two-equation turbulence models need corrections for vortical flows in order to avoid over-prediction of the levels of turbulent viscosity inside vortex cores. In this paper two types of modifications to the two-equation k-omega turbulence model are investigated to overcome this problem. One modification consists of limiting the production of turbulent kinetic energy in the *k*-equation, whereas the other modification is aimed at increasing the production of dissipation in the dissipation equation (omega equation); omega represents the dissipation of turbulent kinetic energy. The computational results at the conditions $M_\infty = 0.85$, $\alpha = 10^o$, and $Re_{c_R} = 9\times10^6$, are compared with detailed experimental surface and field data obtained from a series of wind tunnel tests in the DNW-HST at NLR. The comparisons show that the modification which increases the production term for the dissipation rate of turbulent kinetic energy in the omega-equation produces the best results when it comes to capturing the vortex core in a realistic way. The proposed modification is in line with other approaches found in the literature for one-equation turbulence models.

*) Part of this investigation has been carried out within the framework of WEAG-TA15 under a contract awarded by the Netherlands Agency for Aerospace programs (NIVR) for the Dutch Ministry of Defence, contract number 07601N

Paper presented at the RTO AVT Symposium on "Advanced Flow Management: Part A – Vortex Flows and High Angle of Attack for Military Vehicles", held in Loen, Norway, 7-11 May 2001, and published in RTO-MP-069(I).

Report Documentation Page

Form Approved
OMB No. 0704-0188

Public reporting burden for the collection of information is estimated to average 1 hour per response, including the time for reviewing instructions, searching existing data sources, gathering and maintaining the data needed, and completing and reviewing the collection of information. Send comments regarding this burden estimate or any other aspect of this collection of information, including suggestions for reducing this burden, to Washington Headquarters Services, Directorate for Information Operations and Reports, 1215 Jefferson Davis Highway, Suite 1204, Arlington VA 22202-4302. Respondents should be aware that notwithstanding any other provision of law, no person shall be subject to a penalty for failing to comply with a collection of information if it does not display a currently valid OMB control number.

1. REPORT DATE **00 MAR 2003**	2. REPORT TYPE **N/A**	3. DATES COVERED **-**
4. TITLE AND SUBTITLE **Leading Edge Vortex Flow Computations and Comparisons with DNW-HST Wind Tunnel Data**		5a. CONTRACT NUMBER 5b. GRANT NUMBER 5c. PROGRAM ELEMENT NUMBER
6. AUTHOR(S)		5d. PROJECT NUMBER 5e. TASK NUMBER 5f. WORK UNIT NUMBER
7. PERFORMING ORGANIZATION NAME(S) AND ADDRESS(ES) **NATO Research and Technology OrganisationBP 25, 7 Rue Ancelle, F-92201 Neuilly-Sue-Seine Cedex, France**		8. PERFORMING ORGANIZATION REPORT NUMBER
9. SPONSORING/MONITORING AGENCY NAME(S) AND ADDRESS(ES)		10. SPONSOR/MONITOR'S ACRONYM(S) 11. SPONSOR/MONITOR'S REPORT NUMBER(S)
12. DISTRIBUTION/AVAILABILITY STATEMENT **Approved for public release, distribution unlimited**		
13. SUPPLEMENTARY NOTES **Also see: ADM001490, Presented at RTO Applied Vehicle Technology Panel (AVT) Symposium held inLeon, Norway on 7-11 May 2001, The original document contains color images.**		
14. ABSTRACT		
15. SUBJECT TERMS		

16. SECURITY CLASSIFICATION OF:			17. LIMITATION OF ABSTRACT	18. NUMBER OF PAGES	19a. NAME OF RESPONSIBLE PERSON
a. REPORT **unclassified**	b. ABSTRACT **unclassified**	c. THIS PAGE **unclassified**	**UU**	**14**	

Standard Form 298 (Rev. 8-98)
Prescribed by ANSI Std Z39-18

Introduction

Analysis of vortex dominated flows is of great importance for the assessment of the aerodynamics, the stability and control, the aero-elastics and the structural dynamics of fighter aircraft. The importance of vortex flow to fighter aircraft manifests itself for example as follows:

- Aerodynamics: manoeuvring capabilities depend critically on vortex-induced lift; maximum vortex-induced lift is affected by vortex stability
- Stability and control: the roll stability of complete fighter aircraft can heavily depend on asymmetric vortex breakdown
- Aero-elastics: unsteady vortex flow can affect the flutter speed and the level of limit cycle oscillations
- Structural dynamics: fatigue life of tail surfaces and ventral fins depends significantly on the unsteady aerodynamic energy input to the vibrations of these surfaces; this energy input can be due to vortices.

These observations motivate the investigation of the ability of CFD codes to capture the details of vortical flows around generic configurations like delta wings.

Previous work (see [1], and [2]) shows that the accuracy of CFD predictions for this type of flow and the ability to arrive at a so-called grid-converged solution rely heavily on the ability to represent the turbulent structure of the vortices. Crucial for accurate vortical flow predictions with CFD codes based on the Reynolds-averaged Navier-Stokes (RaNS) equations is the turbulence model used for the computations (see [4]). One- or two-equation turbulence models can potentially reach the required minimum level of modelling. In this paper, new computations are presented for the turbulent vortical flow around a 65° swept cropped delta wing-body configuration with sharp leading edge using a method based on the RaNS equations [4] employing the Wilcox $k-\omega$ two-equation turbulence model [3]. It is well known that present-day one- and two-equation turbulence models require special damping in the vortex cores to represent the effects of fluid rotation (vorticity) as well as 'system' rotation on turbulence. See for example Spalart & Shur [5] and Dacles-Mariani & Zilliac et. al. [6] who proposed modifications to one-equation models, and Hanjalić & Launder [7] for modifications to the ε-equation of the two-equation $k-\varepsilon$ model.

In this paper two types of modifications of the $k-\omega$ two-equation turbulence model are investigated to improve its behaviour for vortical flow simulations. Essentially, these modifications consist of either limiting the production of turbulent kinetic energy or increasing the dissipation rate of turbulent kinetic energy in vortex cores. The results of the computations are compared with detailed experimental data for the sharp-edged delta wing configuration obtained from a series of wind tunnel tests (see [9]). From this comparison the effectiveness of the proposed modifications to the turbulence model is assessed.

The k-ω model and modifications for vortical flows

The Reynolds-averaged Navier-Stokes (RaNS) equations are solved for the conservative (Favre mass-averaged) variables density, ρ, the momentum vector, ρu_j, and the total energy, ρE. In the present study the Wilcox $k-\omega$ turbulence model is considered [3], with the additional 'cross-diffusion' term that has been introduced by Wilcox to decrease the dependency of the solutions on the free-stream value of ω. The transport equations for the turbulent

kinetic energy, k, and the specific turbulent dissipation rate, ω, for the Wilcox model including the so-called cross-diffusion term, to be solved along with the RaNS equations, can be written as (using the summation convention)

$$\frac{\partial(\rho k)}{\partial t}+\frac{\partial(\rho k u_j)}{\partial x_j}=\tau_{ij}^R\frac{\partial u_j}{\partial x_i}-\beta^*\rho\omega k+\frac{\partial}{\partial x_j}[(\mu+\sigma^*\mu_T)\frac{\partial k}{\partial x_j}], \tag{1a}$$

$$\frac{\partial(\rho\omega)}{\partial t}+\frac{\partial(\rho\omega u_j)}{\partial x_j}=\alpha\frac{\rho}{\omega}\tau_{ij}^R\frac{\partial u_j}{\partial x_i}-\beta^*\rho\omega^2+\frac{\partial}{\partial x_j}[(\mu+\sigma\mu_T)\frac{\partial\omega}{\partial x_j}]+\sigma_d\frac{\rho}{\omega}\max\left\{\frac{\partial k}{\partial x_i}\frac{\partial\omega}{\partial x_i},0\right\}, \tag{1b}$$

with t the time, x_i the position vector and μ the molecular dynamic viscosity. The Reynolds-stress tensor τ_{ij}^R is modelled using the Boussinesq hypothesis

$$\tau_{ij}^R=2\mu_T\left(S_{ij}-\frac{1}{3}\frac{\partial u_k}{\partial x_k}\right)-\frac{2}{3}\rho k\delta_{ij}, \tag{2}$$

with S_{ij} the rate-of-strain tensor $S_{ij}=\frac{1}{2}(\partial u_i/\partial x_j+\partial u_j/\partial x_i)$.

The turbulent (eddy) viscosity μ_T is defined by

$$\mu_T=\alpha^*\frac{\rho k}{\omega}. \tag{3}$$

The first two terms on the right hand sides of both the k -equation (1a) and the ω -equation (1b) represent production and dissipation of k and ω, respectively. If we define the rate-of-strain tensor with zero trace as $\tilde{S}_{ij}=S_{ij}-\frac{1}{3}D\delta_{ij}$, where the dilatation is defined by $D=\partial u_i/\partial x_i$, and if we define the magnitude of this rate-of-strain tensor as $\tilde{S}=\{2\tilde{S}_{ij}\tilde{S}_{ij}\}^{1/2}$, then the production terms can be written as

$$\begin{aligned}P_k&=\tau_{ij}^R\frac{\partial u_j}{\partial x_i}=\mu_T\tilde{S}^2-\frac{2}{3}\rho kD,\\ P_\omega&=\alpha\frac{\omega}{k}\tau_{ij}^R\frac{\partial u_j}{\partial x_i}=\frac{\alpha\omega}{k}P_k=\alpha\alpha^*\rho\tilde{S}^2-\frac{2}{3}\alpha\rho\omega D.\end{aligned} \tag{4}$$

The dissipation term in the k -equation is usually denoted by $\rho\varepsilon=\beta^*\rho\omega k$. The last term on the right hand side of the ω -equation in (1a) is the so-called cross-diffusion term mentioned above. The values of the coefficients are taken as the high Reynolds number limits for the $k-\omega$ model as presented in [3]:

$$\alpha^*=1,\ \alpha=0.5,\quad \beta^*=0.09,\quad \beta=0.075,\quad \sigma^*=1,\quad \sigma=0.6,\quad \sigma_d=0.3. \tag{5}$$

It is shown by Kok (see [8]) that with the 'cross-diffusion' term included the dependency on free-stream values can be completely removed with the following values for the coefficients of the diffusion terms: $\sigma^*=2/3$, $\sigma=0.5$, $\sigma_d=0.5$, called the 'TNT set'. However, for the computations presented here, still the 'Wilcox set' of coefficients (5) is used. In order to avoid unphysical production of eddy viscosity in regions of stagnating flow, the production of turbulent kinetic energy is limited with a commonly used standard limiter relating the maximum allowable production to the dissipation of turbulent kinetic energy

$$P_k=\min\{P_k^u,20\rho\varepsilon\}, \tag{6}$$

with P_k^u the unlimited production defined by (4). In the discussion that will follow the model as described above will be referred to as 'standard $k-\omega$ model' in order to distinguish it from the modified versions discussed below.

It is well known that most one- and two-equation models produce too much eddy viscosity in vortices causing a far too strong diffusion of vorticity. For the Baldwin-Barth and the Spalart-Allmaras one-equation models, modifications were proposed by Dacles-Mariani et al. (see [6]) and by Spalart & Shur (see [5]) to cure this problem. Both modifications use the ratio *r* of the magnitude of the rate-of-strain tensor and the magnitude of vorticity $\Omega = \{2\Omega_{ij}\Omega_{ij}\}^{1/2}$, with the vorticity tensor $\Omega_{ij} = \frac{1}{2}(\partial u_j/\partial x_i - \partial u_i/\partial x_j)$, $r = \tilde{S}/\Omega$. In shear layers, the velocity gradient is dominated by the gradient in the normal direction, so that $r \approx 1$. In the core of a vortex, the flow approaches pure rotation, implying that $r << 1$. In the one-equation models, a PDE for the eddy viscosity is defined. In the modifications of Dacles-Mariani et al. [6] and of Spalart & Shur [5] the production of eddy viscosity in this equation is essentially modified by multiplication with a function *f(r)*. This function has the properties $f(1) = 1$, so that the production is unchanged in boundary layers, and $f(r) < 1$ for $r < 1$, so that the production is reduced in vortex cores. The modified production term is given by $P_{\nu_T} = C_1 \rho \nu_T \Omega f(r)$ with C_1 a (positive) constant and $\nu_T = \mu_T / \rho$.

In order to improve the behaviour of the $k-\omega$ model for vortex dominated flows we have considered two modifications of the source terms depending on the variable *r*. The first modification is an extension of the limiting of the *k*-production as done in equation (6) using the dissipation term as a limiter but now with the coefficient being a linear function of *r*,

Modification 1: $$P_k = \min\left\{P_k^u, (C_{k1} + C_{k2}\min\{0, r-1\})\rho\varepsilon\right\}, \qquad (7)$$

with $C_{k1} > 1$ and $C_{k2} > 0$. In this way the *k*-production is reduced or even turned into a dissipation term inside vortex cores. For boundary layers, however, taking a value of C_{k1} close to 1 may also result in a reduction of the production, if the boundary layer is not in equilibrium (balance between production and dissipation). For this type of modification we have investigated two choices for the parameters. In both cases $C_{k1} = 2.0$ is taken whereas the value of the coefficient of the r-dependent part is set to $C_{k2} = 2.0$ and $C_{k2} = 8.0$, respectively. In the second modification of the $k-\omega$ model, we have left the production term of the *k*-equation unchanged (in which, in fact, the only modelling assumption is the Boussinesq hypothesis), and modified the production term of the ω-equation as follows,

Modification 2: $$P_\omega = \alpha\alpha^* \rho \max\{\Omega^2, \tilde{S}^2\}, \qquad (8)$$

which is equivalent to dividing the production term in the ω-equation by $\min\{r^2, 1\}$, and where a non-zero dilatation has been neglected. In this way, the production of ω is increased in vortex cores, thus increasing the dissipation of turbulent kinetic energy and, as a consequence, a reduction of the production of eddy viscosity is obtained. From the *k*-equation and the modified ω-equation, an equation for the eddy viscosity can be derived for which the production is now of the form $P_{\nu_T} = (1-\alpha)\alpha^* \rho \nu_T \Omega^2 f(r)/\omega$, with $f(r) = [r^2 - \alpha \max\{r^2, 1\}]/(1-\alpha)$, which shows some similarities with the expressions used by Spalart & Shur [5] and Dacles-Mariani et al. [6] for one-equation turbulence models mentioned above. Furthermore, the second type of modification is quite similar to the

modification of Hanjalić & Launder [7] who propose to introduce a term proportional to $k\Omega^2$ in the ε-equation of the $k-\varepsilon$ two-equation model. However, Hanjalić's term has a sign opposite to the present proposal.

Test case

As a test case for the present study the flow around a 65° cropped delta wing with sharp leading edge is used. The wing is the same as the one that has been the subject of the 'International Vortex Flow' experimental study reported in [9]. The balance mounted delta wing model was measured in different wind tunnels and the experimental data were aimed to set up an experimental data base for the validation of Euler codes to be used for the prediction of vortical flow characteristics in the subsonic and transonic speed regime. In 1988 NLR manufactured a new model with the same geometry (the sharp edge variant) with a very dense matrix of pressure taps. Since then this model, which will be referred to as the WB1-SLE model, has been the subject of five test programs in the DNW-HST facility at NLR throughout the years. All five tests were aimed at getting detailed experimental data to be used for validation purposes for CFD codes capturing the characteristics of various aspects of vortical flows. The first test during which detailed surface pressure measurements and surface flow visualisations for symmetric (no side-slip) subsonic and transonic conditions have been obtained are reported in [10]. The tests that followed included a flow field investigation using a 5-hole pressure probe at a subsonic and a transonic condition, where a number of cross-flow planes have been surveyed, and investigations into asymmetric flow (side-slip angle sweeps). Also a flow field investigation with the Particle Image Velocimetry (PIV) technique at a subsonic and a transonic condition, focussing on the angle of incidence / slip-angle combinations where transition to vortex breakdown takes place, has been carried out. An overview of the tests and an analysis of all experimental data obtained in the different tests are given in [11]. The basic chordwise wing sections of the sharp-edged delta wing are defined by the NACA64a005 profile. Between the leading edge and the 40% chord line the geometry is changed into two circular arcs, defining the sharp leading edge. Between the 75% chord line and the trailing edge the geometry is replaced by a straight-line blend towards the trailing edge (see Figure 1). The wing is mounted on an underwing fuselage that has served in the wind tunnel experiments as the support for the instrumentation of the model. An impression of the complete model is shown in Figure 1. The flow case considered in the present study is the transonic flow around the sharp edged delta wing (WB1-SLE) for a Mach number of $M_\infty = 0.85$, an angle of incidence of $\alpha = 10^o$, and a Reynolds number based on the root chord, c_R, of $Re_{c_R} = 9\times10^6$. At these conditions detailed surface pressure measurements are available from the DNW-HST experiments as well as flow-field data in three cross-flow planes obtained with the 5-hole pressure probe as mentioned above.

CFD method and computational grid

Computations have been performed using the flow solver *ENSOLV*, that is part of NLR's *ENFLOW* system for flow simulations based on the Euler- or the Navier-Stokes equations (see [12]). A cell-centred, central difference, finite volume scheme is used to discretize the RaNS equations in space, where high-aspect-ration scaling of the artificial dissipation, and a matrix dissipation formulation used in surface normal direction are applied. The turbulence equations are discretized in the same way as for the basic flow equations, where it should be noted that for the turbulence model equations a TVD switch is used in the formulation of the artificial dissipation leading to a second order TVD scheme for these equations. It should be mentioned that for the implementation of the $k-\omega$ model the

equations are reformulated such that instead of ω a newly introduced quantity $\tau = 1/(\omega + \omega_0)$ is used as the second turbulence variable, removing the singular behaviour of the solution at solid walls (see [12]). The turbulence variables k and τ are both set to zero at solid walls. At the 'inflow' parts of the far field boundaries the free-stream values for the turbulence variables are computed from specified values of the free-stream turbulence Reynolds number and the free-stream dimensionless turbulent kinetic energy (set to 0.01 and 10^{-6}, respectively).

A suitable computational grid has been defined using the domain modeller ENDOMO and the grid generation program ENGRID, both programs being part of NLR's ENFLOW flow simulation system (see [12]). A CO-type topology has been used with a singular line running from the apex to the upstream far-field boundary, where an O-type singularity occurs at the edges of the wake-cut downstream of the trailing edge towards the downstream far-field boundary. It has been demonstrated before (see for example [1] and [2]) that this type of topology allows for grids that are very well suited for the flow under consideration, which is expected to be conical over large part of the delta wing. The computations have been carried out for the half model due to the symmetric flow conditions. The far-field boundary is placed at approximately 3 root chords from the geometry. The grid consists of 145∗153∗81 = 1,796,985 grid points. A rather fine mesh spacing has been used in spanwise direction (152 cells distributed over upper wing, lower wing and fuselage) to be able to capture the vortex structures in an accurate way**.** For the 81 points in normal direction it is checked with the computed results that about 30 to 35 points are located in the boundary layer. Furthermore it has been checked that for almost the entire wing- and fuselage surface the dimensionless (based on the friction velocity) height of the first cell normal to the wall is in the range of $0.5 < y^+ < 1.0$. An impression of the computational grid is given in Figure 2.

Discussion of results

The pressure coefficients on the upper wing surface computed with the NLR implementation of the $k-\omega$ model and its modifications are compared with experimental data in Figure 3. The experimental data indicate a primary vortex of which the 'footprint' is visible in the region of high suction and a pressure plateau between the footprint and the leading edge. The standard NLR $k-\omega$ model results obviously do not represent this situation. Only a small region indicating vortex formation close to the wing apex is visible (probably caused by a separation of the locally laminar flow) after which the primary separation covers the entire region between the location of the suction rise and the leading edge. In Figure 4 the upper surface limiting streamlines for the different computations are compared. All computational results show a primary separation over the entire leading edge attaching at similar positions (A_1 in Figure 4). The results obtained with the modifications of the $k-\omega$ model show a secondary separation (S_2) underneath the primary vortex that attaches again outboard of the secondary separation line. This secondary separation, also observed in the experiments, is missing in the results obtained with the standard $k-\omega$ model. This is due to the fact that with the standard NLR $k-\omega$ model, a large amount of turbulent kinetic energy is produced inside vortices. This high level of turbulence strongly diffuses the vorticity and dissipates some of the kinetic energy associated with the swirling flow component of the vortex. The results obtained with the subsequent modifications of the turbulence model differ in the location of the secondary separation, S_2, and the location of the secondary reattachment, A_2. However, the location of the primary reattachment, A_1, is close to the experimentally observed position as can be determined from the sectional pressure distributions presented in Figure 5 and Figure 6. It is

observed there that the location of the primary reattachment in the result obtained with the standard NLR $k-\omega$ model is too far inboard as compared with the experimental data. The locations for primary reattachment and secondary separation shown for the experiment are derived from oil flow visualisations. From the pressure distributions it can be seen that all the modifications constitute a strong improvement over the standard model. For the modification using the limiter for the k - production term with a coefficient of $C_{k2}=8$, however, the reduction of turbulence production has been exaggerated, resulting in a large over-prediction of the suction peak. The other two results are close to each other and to the experimental results. In particular, the width of the suction peak and the pressure plateau between the peak and the leading edge are predicted well. The main difference between the P_k - limiter and the P_ω - modification approach is the way the pressure distribution changes in downstream direction. With the P_k -limiter approach (with $C_{k2}=2$), the height of the suction peak gradually drops compared to the P_ω - modification approach and the experimental data. In order to investigate the behaviour of the two most promising modifications models further, we have looked at the downstream development of the distribution of the total-pressure-loss Figure 7 and of the turbulence Reynolds number $Re_T=\rho k/\{\omega\mu\}$ Figure 8. For both modifications, the total pressure loss shows a fairly strong primary vortex with mild secondary separation. Moving in downstream direction, the primary vortex obtained with the P_k -limiter approach appears to become more diffuse than the results obtained with the P_ω - modification approach. This is related to the distribution of the turbulence Reynolds number, where we see that for the P_k -limiter modification, the turbulence Reynolds number increases strongly in downstream direction, while this increase is lower for the P_ω - modification. Furthermore, the distribution of the turbulence Reynolds number obtained with the P_ω - modification shows for each section a local minimum in the vortex core. In particular this last observation is important, since it is known from theory that a turbulent vortex can have a laminar core if the fluid rotation becomes strong enough. In Figure 9computed total-pressure-losses are compared in detail with experimental field data for a cross-flow plane (normal to the free stream direction) at 90% root chord position. Again it is clear that the standard NLR implementation of the $k-\omega$ model generates a far more diffuse vortex. Both modifications presented for the $k-\omega$ model show qualitatively the same vortex structure as in the experiment. Differences between the modifications of the $k-\omega$ model become most clear when looking at the total-pressure-loss distribution along a horizontal traverse and a vertical traverse through the primary vortex core in these planes. The comparison is made as a function of the dimensionless distance from the primary vortex core for each solution. In this way a difference in location of the vortex core in the solutions does not show up and only the difference in total-pressure-loss distributions within the vortex is judged upon. It can be seen that compared with the experiment all modifications over-predict the level of total-pressure-loss in the vortex core. However, it is concluded that with respect to the downstream development of the size of the vortex as well as for the levels of total-pressure-losses in the region just outside the core the P_ω - modification gives the best results as compared with the experiment. Comparisons of ‘in-plane’ velocity components at a cross-flow plane normal to the free stream direction at 97% chordwise position in Figure 10 supports this observation. Especially the distribution of the vertical velocity component along a horizontal traverse through the vortex core as obtained with the P_ω - modification is in good agreement with the experimental data at this station.

Concluding remarks

Computations have been performed for the turbulent vortical flow over a sharp-edged cropped delta-wing / underwing-fuselage configuration with the ENFLOW Navier-Stokes method. The computations have been carried out on a computational grid of relatively high resolution consisting of 1,796,985 grid points. The computations have been carried out at a transonic free-stream Mach number of 0.85, an angle of incidence of 10 degrees and a Reynolds number of 9 million. The purpose of the computations is to investigate the capability of different modifications of a two-equation turbulence model to improve predictions of turbulent vortical flow. Results obtained with the NLR implementation of the Wilcox $k-\omega$ turbulence model (including the 'cross-diffusion' term, [12]), and two modifications for vortical flow to this $k-\omega$ model, have been presented. One of these modifications is aimed at reducing the unphysical high production of turbulent kinetic energy in the vortex core predicted with the standard $k-\omega$ model and has been tested for two combination of the its parameters. The second modification basically has the same effect but accomplishes this effect by increasing the production of ω in vortex cores. Based on detailed comparison with experimental data for this case the following conclusions are drawn:

- Standard $k-\omega$ models produce unphysical high levels of turbulent viscosity inside vortex cores, resulting in vorticity diffusion that is larger than found in experiments.
- The modification based on increasing the ω-production term is demonstrated to produce the best agreement with experimental surface pressure and flow-field data. This modification also is the only one that maintains a local minimum of the turbulence Reynolds number at the vortex centre throughout the flow, which agrees with the theoretical observation that turbulent vortices can have a laminar sub-core.
- The approach to modify the ω-equation seems consistent with approaches adopted by other authors to modify one-equation turbulence models for vortical flow simulations.

It is recognised that there is still a need for a better theoretical foundation of modifications to the ω-equation to properly account for high levels of vorticity. Although detailed experimental data have been used in the present paper more complete information on the turbulence in vortex cores is required, generated either by DNS or LES simulations of vortex cores or new dedicated experiments (see for example [13]).

References

[1] Brandsma, F.J., and Sytsma, H.A., Navier-Stokes Computations for a Round-Edged Delta Wing; Influence of underwing body, grid density, and laminar turbulent transition location, NLR CR 97490 L, 1997.

[2] Arthur, M.T., Kordulla W., Brandsma, F.J., and Ceresola, N., Grid adaptation in vortical flow simulations, AIAA 15th Applied Aerodynamics Conference, Atlanta GA, USA, June 1997.

[3] Wilcox, D.C., A Two-Equation Turbulence Model for Wall-Bounded and Free-Shear Flows, AIAA-93-2905, AIAA 24th Fluid Dynamics Conference, Orlando, July 6-9, 1993.

[4] Kok, J.C., Brandsma, F.J., Turbulence Model based Vortical Flow Computations for a Sharp Edged Delta Wing in Transonic Flow using the full Navier-Stokes Equations, NLR-CR-2000-342, 2000.

[5] Spalart, P.R. and Shur, M., On the Sensitization of Turbulence Models to Rotation and Curvature, Aerospace Science and Technology, No. 5, pp.297-302, 1997

[6] Dacles-Mariani, J. and Zilliac, G.G., Numerical/Experimental Study of a Wingtip Vortex in the Near Field, AIAA Journal, Vol. 33, No. 9, pp. 1561-1568, 1995.

[7] Hanjalić, K., Launder, B.E., Sensitizing the Dissipation Equation to Irrotational Strains, ASME J. Fluids Eng., Vol. 102, pp. 34-40, 1980.

[8] Kok, J.C., Resolving the dependence on free-stream values for the k-ω turbulence model. NLR-TP-99295, 1999 (also AIAA Journal, July 2000).

[9] Elsenaar, A., et.al., The International Vortex Flow Experiment, AGARD CP 437, Validation of Computational Fluid Dynamics, May 1988.

[10] Elsenaar A., Hoeijmakers, H.W.H.M., An experimental study of the flow over a sharp edged delta wing at subsonic and transonic speeds, AGARD CP-494, Vortex Flow Aerodynamics, Paper 15, 1991.

[11] Boersen, S.J., Analysis of surface pressure and flow field measurements on the WB1-SLE configuration (65° sharp-edged cropped delta wing) at subsonic and transonic speeds in the DNW-HST, NLR-CR-99525, 1999.

[12] Kok, J.C., Spekreijse, S.P., Efficient and accurate implementation of the k-ω turbulence model in the NLR multi-block Navier-Stokes system, presented at the ECCOMAS 2000 Conference, Barcelona, Spain, 11-14 September 2000, NLR-TP-2000-144.

[13] Riley, A.J., Lowson, M.J., Development of a three-dimensional free shear layer, J. of Fl. Mech., Vol. 369, pp.48-89, 1998.

Figures

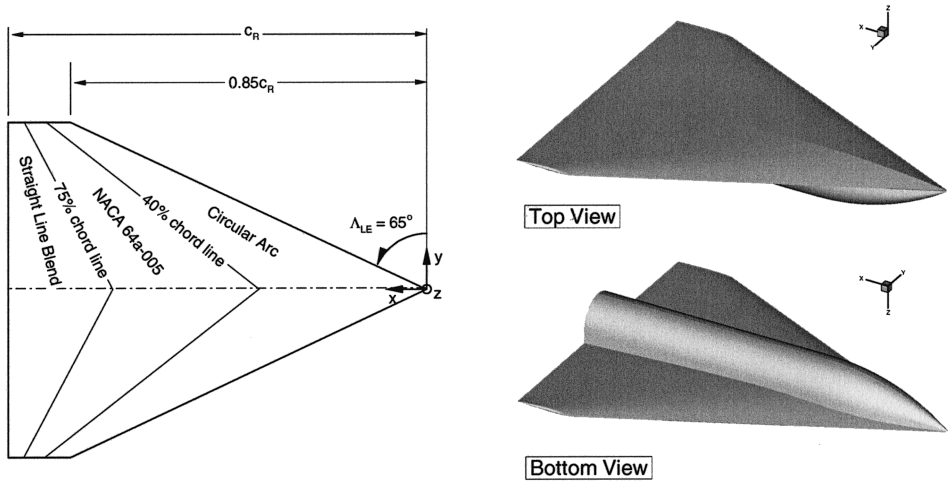

Figure 1 Definition of the 65° cropped sharp-edged delta wing and impression of the windtunnel model geometry

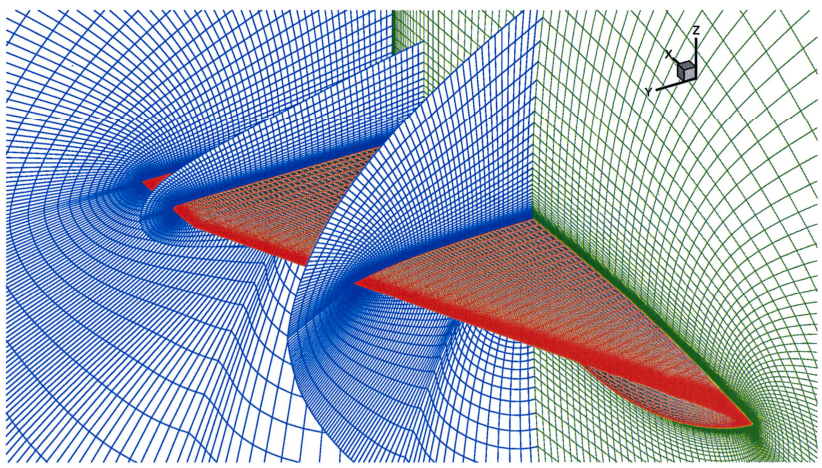

Figure 2 Impression of the computational grid (surface, symmetry plane and cross-flow grid planes)

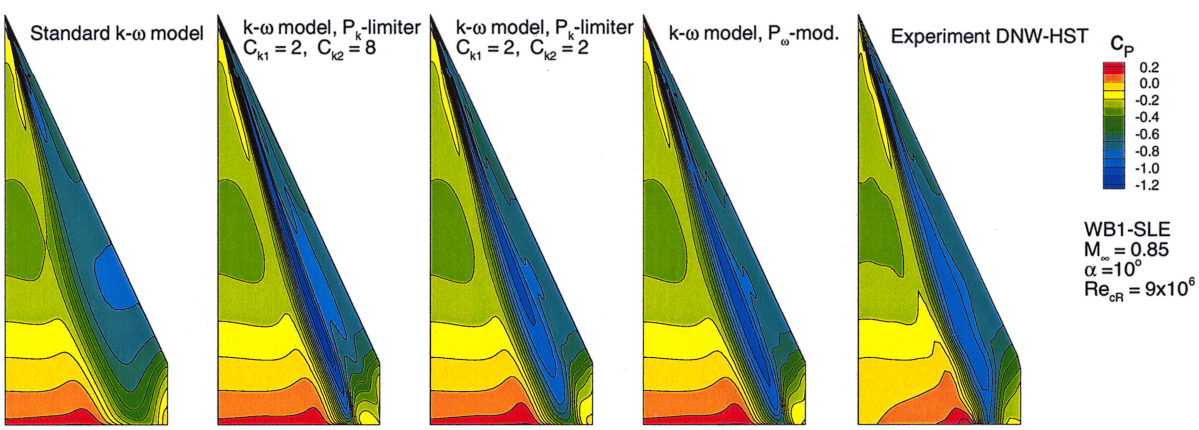

Figure 3 Comparison of upper-surface pressure distributions (half wing)

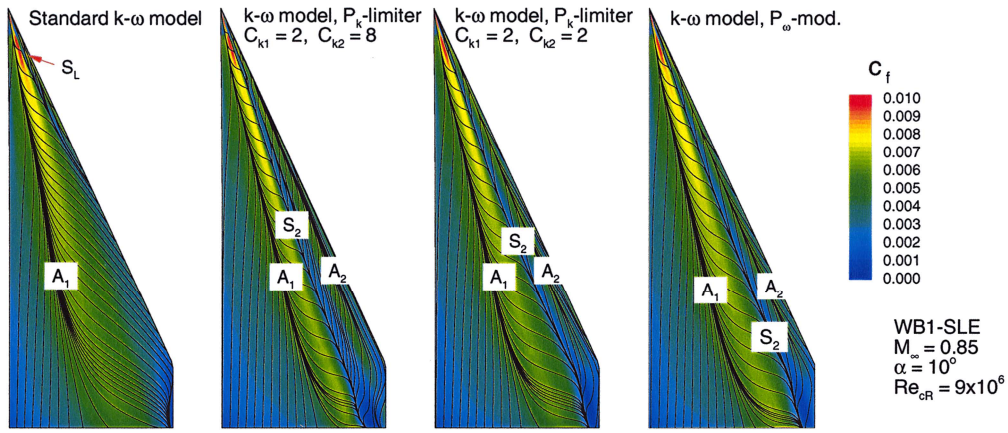

Figure 4 Upper surface limiting streamlines and skin friction distributions

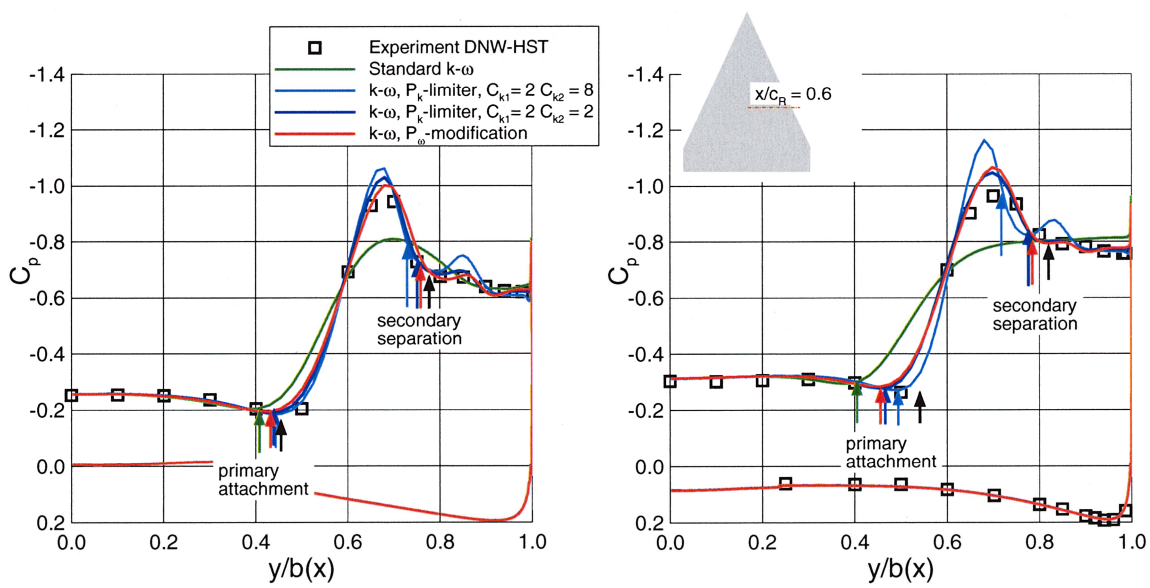

Figure 5 Comparison of spanwise pressure distributions

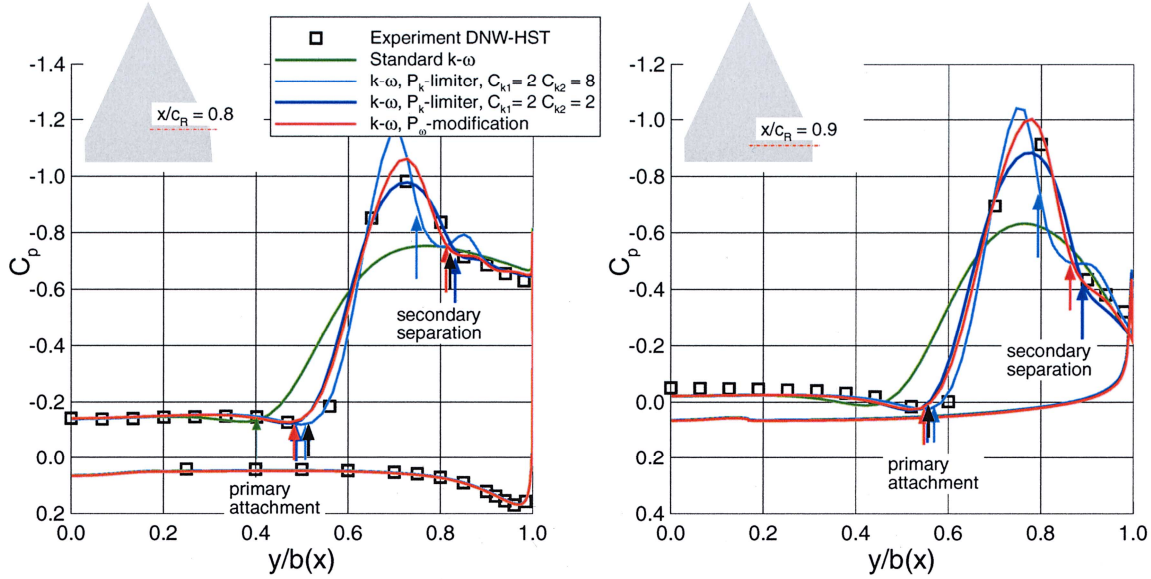

Figure 6 Comparison of spanwise distributions

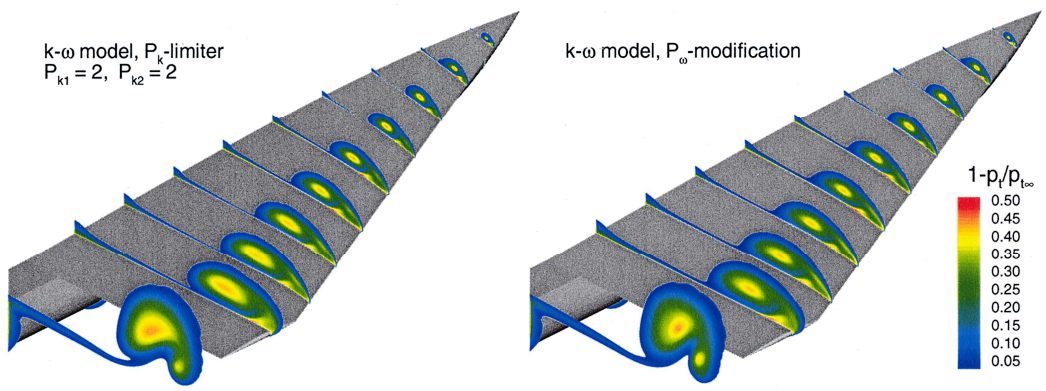

Figure 7 Total pressure loss distribution in cross-flow planes

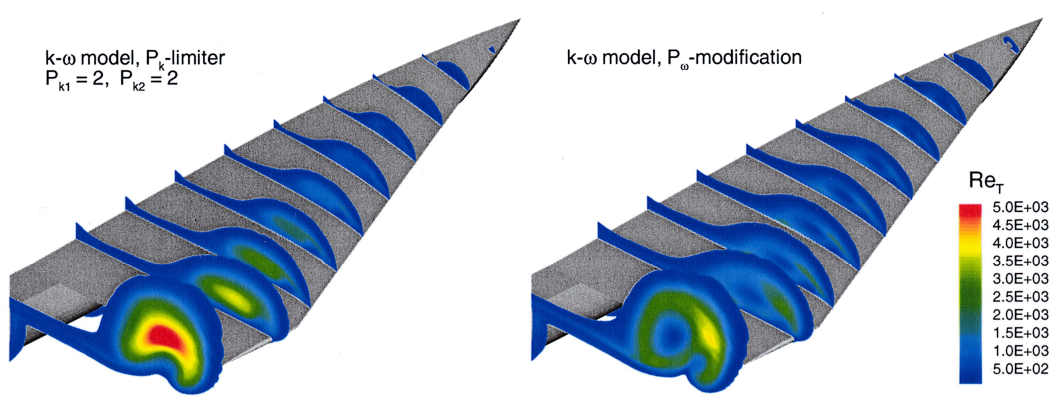

Figure 8 Turbulence Reynolds number distribution in cross-flow planes

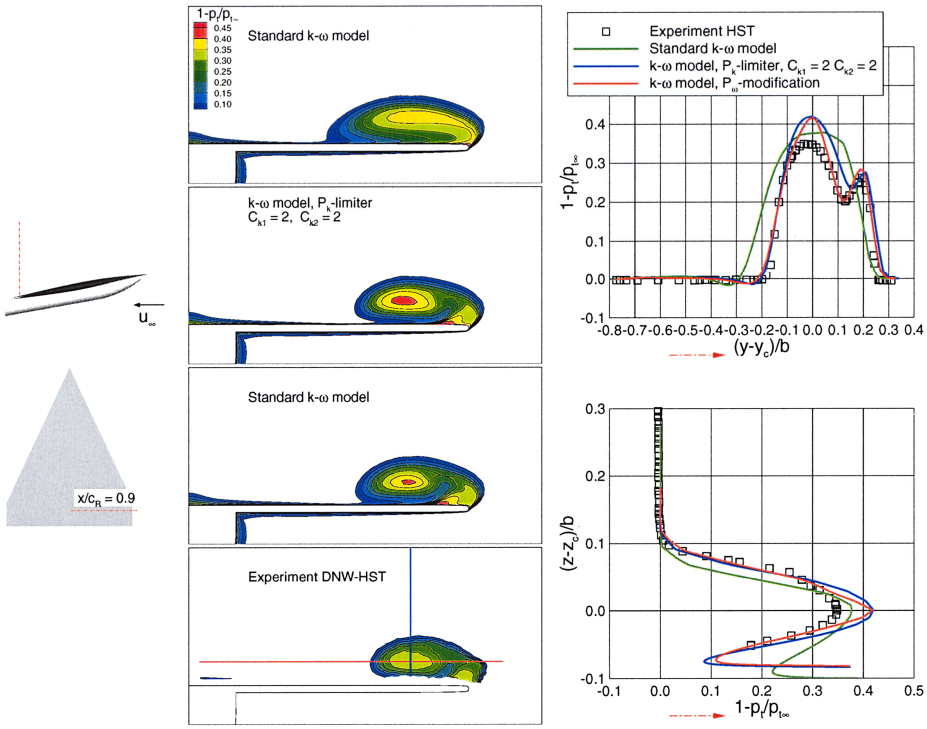

Figure 9 Comparison of of total pressure losses in a cross-flow plane at $x / c_R = 0.9$ with experimental data

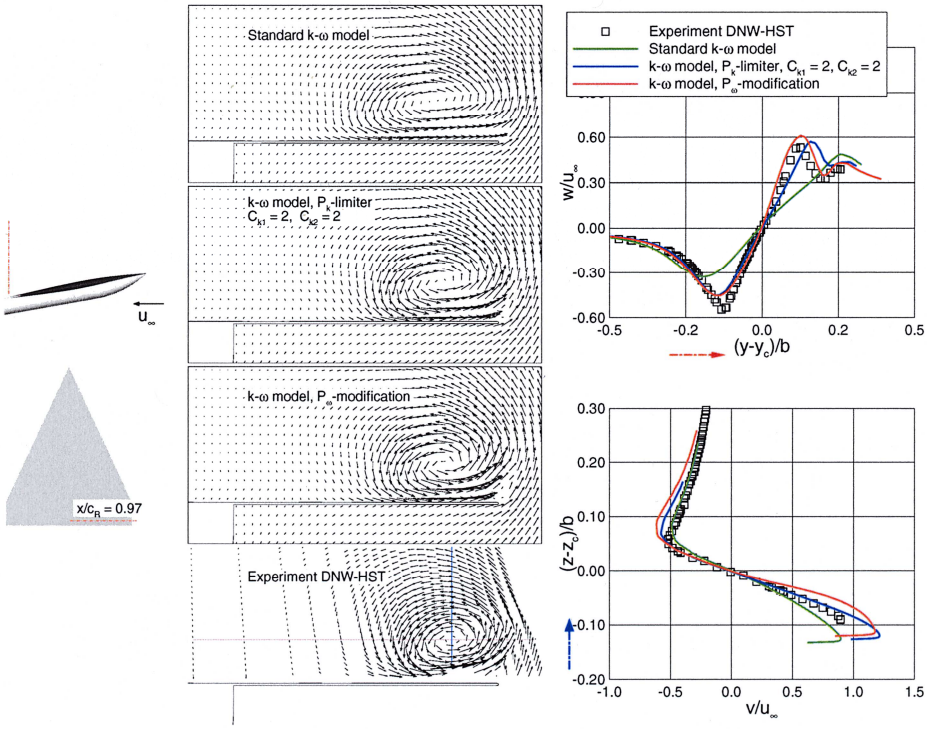

Figure 10 Comparison of in-plane velocity components in a cross-flow plane at $x / c_R = 0.97$ with experimental data

This page has been deliberately left blank

Page intentionnellement blanche